J Inorg Organomet Polym (2014) 24:803–818
DOI 10.1007/s10904-014-0046-8

Synthesis, Thermal and Morphological Properties of Polyurethanes Containing Azomethine Linkage

Musa Kamacı · İsmet Kaya

Received: 20 March 2014 / Accepted: 26 May 2014 / Published online: 14 June 2014

Abstract This paper presents synthesis, photophysical, electrochemical, thermal and morphological properties of Schiff bases containing various side-group substitutions and polyurethanes (PUs) containing azomethine linkage. Morphological properties of PUs containing azomethine bonding were investigated by scanning electron microscopy (SEM). SEM images showed that PU containing azomethine consist of semi-crystalline particles. Thermal transitions in PUs containing azomethine units were studied using DSC. The obtained DSC curves showed that PUs containing azomethine are semi-crystalline materials due to they contain both crystallization and melting peaks. Electrochemical properties also investigated by using cyclic voltammetry (CV). According to the cyclic voltommagrams and CV data, PUs containing azomethine have below 2.0 eV electrochemical band gap.

Keywords Semi-crystalline polymer · Low-band gap polymers · Electrochemical and morphological properties · Thermal analysis

1 Introduction

Over the past years, conjugated polymers have attracted widespread interest both academic and industrial application because of their useful electronic, optoelectronic, electrochemical and non-linear optical properties [1]. They have potential application such as polymer light-emitting diodes (PLEDs) [2], polymer solar cells (PSCs) [3], and organic field-effect transistors (OFETs) [4]. In addition, they have several advantages such as low cost, lightweight, good flexibility, readily processed and easily printed [5]. There are many prototypical conjugated polymers, such as polyacetylene, poly(*p*-phenylene) and poly(*p*-phenylene-vinylene) [6]. Polymeric Schiff bases, which also known polyazomethines (PAMs), are another class of conjugated polymers. They contain one or more imine (–N=CH) linkages in the structures. In addition, they exhibit good thermal stability [7], excellent mechanical strength [8], metal-chelating ability [9], and, in some cases, liquid crystalline morphology [10].

Polyurethanes (PUs) are another important class of polymers due to they have found a widespread use in the medical, automotive and industrial fields [11]. PUs represent a complex group of synthetic polymers and they can be found in almost every aspect of our lives, such as adhesives, in flexible foams, covers, fibers, medical devices and tissue scaffolds [12–15]. PUs containing azomethine, which are also known poly(azomethine-urethane)s (PAMUs), were also reported in literature and their thermal stability [16], semi-crystalline behavior [17], non-linear optical properties [18], electrochemical properties [19], solar cell application [20] and ion sensor application [21, 22] were clarified. To the best of our knowledge, there is not too much paper in the literature on PUs containing azomethine.

2 Experimental Section

2.1 Materials

4-Hydroxy benzaldehyde (4-DHBA), *o*-phenylenediamine (*o*-PDA), 4-methyl-*o*-phenylenediamine (*o*-PDAM), 4-nitro-

M. Kamacı · İ. Kaya (✉)
Polymer Synthesis and Analysis Lab., Department of Chemistry, Faculty of Sciences and Arts, Çanakkale Onsekiz Mart University, 17020 Çanakkale, Turkey
e-mail: kayaismet@hotmail.com

M. Kamacı
Department of Chemistry, Faculty of Sciences and Arts, Piri Reis University, Tuzla, 34940 Istanbul, Turkey

o-phenylenediamine (*o*-PDAN), 2,4-toluene diisocyanate (TDI), hexamethylene diisocyanate (HDI), dimethylformamide (DMF), dimethylsulfoxide (DMSO), tetrahydrofurane (THF), methanol (MeOH), ethanol (EtOH), acetone, acetonitrile (MeCN), toluene, ethyl acetate, $CHCl_3$, CCl_4 and *n*-hexane were supplied from Merck Chemical Co. (Germany).

2.2 Synthesis of Schiff Bases

Schiff base abbreviated as 4-DHBA-*o*-PDA, 4-DHBA-*o*-PDAM and 4-DHBA-*o*-PDAN, and they were synthesized by the condensation reactions of 4-DHBA with *o*-PDA, *o*-PDAM or *o*-PDAN as in the literature [23]. Synthesis procedure of Schiff bases was as follows: 4-DHBA (3.664 g, 3.00×10^{-2} mol) was dissolved in 30 mL MeOH and added into a 250 mL three-necked round-bottom flask, which was fitted with condenser, thermometer and magnetic stirrer. Reaction mixture was heated up to 50 °C and then *o*-PDA (1.622 g, 1.5×10^{-2} mol), *o*-PDAM (1.833 g, 1.5×10^{-2} mol) or *o*-PDAN (2.297 g, 1.5×10^{-2} mol) in 20 mL MeOH was added into the flask. Reaction was maintained for 3 h under reflux, and cooled at the room temperature. The obtained Schiff bases were washed MeCN (2×50 mL) and water (2×100 mL) to remove the unreacted components. The product was dried in a vacuum oven at 75 °C for 24 h. The yields of 4-DHBA-*o*-PDA, 4-DHBA-*o*-PDAM and 4-DHBA-*o*-PDAN were found as 73, 79 and 75 %, respectively.

2.3 Synthesis of PUs Containing Azomethine

PAMUs were synthesized by the step-polymerization reaction of the preformed Schiff bases with aliphatic (HDI) or aromatic (TDI) diisocyanates. They were also abbreviated as 4-DHBA-*o*-PDA-TDI, 4-DHBA-*o*-PDAM-TDI, 4-DHBA-*o*-PDAN-TDI, 4-DHBA-*o*-PDA-HDI, 4-DHBA-*o*-PDAM-HDI and 4-DHBA-*o*-PDAN-HDI. Synthesis procedure of PUs containing azomethine units is as follows: 4-DHBA-*o*-PDA (0,633 g, 2×10^{-3} mol), 4-DHBA-*o*-PDAM (0.661 g, 2×10^{-3} mol) or 4-DHBA-*o*-PDAN (0.723 g, 2×10^{-3} mol) were dissolved in 60 mL DMF/THF (1/3) mixture and added into a 250 mL three-necked round-bottom flask which was fitted with condenser, magnetic stirrer, and inert gas supplier. Reaction mixtures were heated up to 60 °C and TDI (0.348 g, 2×10^{-3} mol) or HDI (0.336 g, 2×10^{-3} mol) was dissolved in 50 mL THF, and added into the flask. Reactions were maintained for 6 h under Argon atmosphere, cooled at the room temperature, and kept for 24 h. The obtained PAMUs were washed by MeOH (2×50 mL) and MeCN (2×50 mL) to remove the unreacted components. The products were dried in a vacuum oven at 75 °C for 24 h [19]. The yields of 4-DHBA-*o*-PDA-TDI, 4-DHBA-*o*-PDAM-TDI, 4-DHBA-*o*-PDAN-TDI, 4-DHBA-*o*-PDA-HDI, 4-DHBA-*o*-PDAM-HDI and 4-DHBA-*o*-PDAN-HDI were found as 93, 87, 84, 86, 82 and 83 %, respectively. All the synthesis procedures were summarized in Scheme 1.

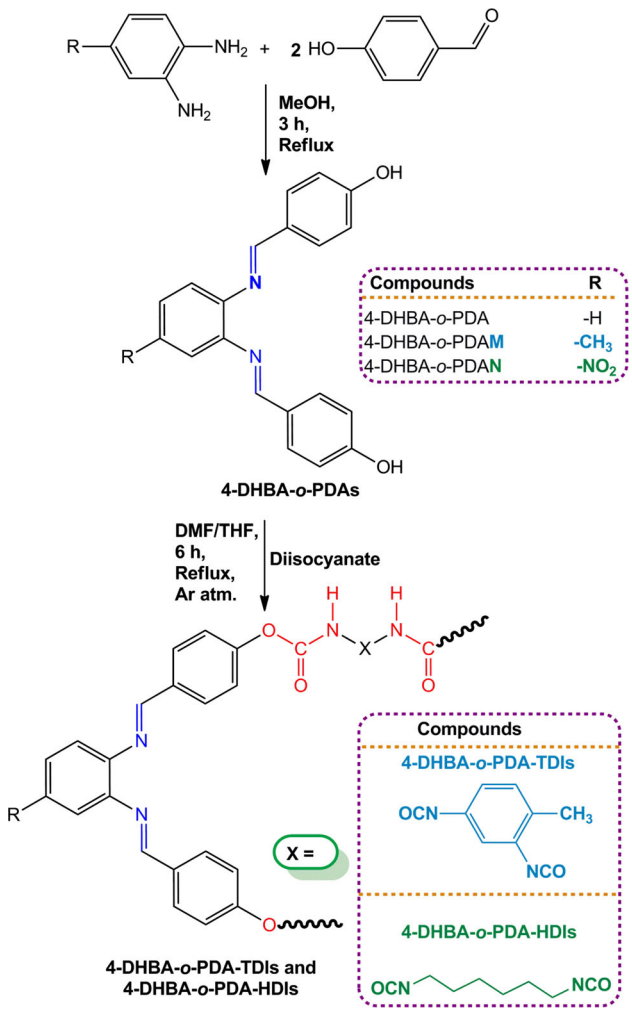

Scheme 1 Synthesis of Schiff bases and PUs containing azomethine unit

2.4 Characterization Techniques

The solubility tests were done in different solvents by using 1 mg sample and 1 mL solvent at 25 °C. The prepared compounds were characterized by using FT-IR, ^{1}H-NMR, ^{13}C-NMR spectra and size exclusion chromatography (SEC). The infrared spectra were obtained by Perkin Elmer FT-IR Spectrum one using universal ATR sampling accessory (4,000–550 cm^{-1}). ^{1}H-NMR and ^{13}C-NMR spectra (Bruker AC FT-NMR spectrometer operating at 400 and 100.6 MHz, respectively) were recorded in deuterated DMSO-d_6 at 25 °C. Tetramethylsilane (TMS) was used as internal standard. The number-average molecular weight (Mn), weight-average molecular weight (Mw) and

polydispersity index (PDI) were determined by SEC technique of Shimadzu Co. For SEC investigations, an SGX (100 Å and 7 nm diameter loading material) 3.3 mm i.d. × 300 mm columns was used; eluent: DMF (0.4 mL/min), polystyrene standards were used. A refractive index detector (RID) was used to analyze the products at 25 °C.

2.5 Photophysical Properties

Ultraviolet–visible (UV–Vis) spectra were measured by Analytikjena Specord 210 Plus at 25 °C using DMSO. The optical band gaps (E_g) were calculated from the absorption edges as in the literature [24]. A Shimadzu RF-5301PC spectrofluorophotometer was used in fluorescence measurements. Photoluminescence (PL) spectra were obtained in DMF solutions. Solution concentrations of the spectrofluorophotometer were adjusted to between 2.00×10^{-1}–6.25×10^{-2} mg/L and slit = 3 nm for all measurements, respectively.

2.6 Electrochemical Properties

Cyclic voltammetry (CV) measurements were carried out with a CHI 660C Electrochemical Analyzer (CH Instruments, TX, USA) at a potential scan rate of 20 mV/s. All the experiments were performed in a dry box filled with argon at room temperature. The system consisted of a CV cell containing glassy carbon (GCE) as the working electrode, platinum wire as the counter electrode, and Ag wire as the reference electrode. The electrochemical potential of Ag was calibrated with respect to the ferrocene/ferrocenium (Fc/Fc^+) couple. The half-wave potential ($E^{1/2}$) of (Fc/Fc^+) measured in MeCN solution of 0.1 M tetrabutylammonium hexafluorophosphate ($TBAPF_6$) MeCN solution is 0.39 V with respect to Ag wire. The voltammetric measurements were carried out in MeCN/DMSO mixtures (v/v: 3/2). The HOMO–LUMO energy levels and electrochemical band gaps (E'_g) were calculated from the oxidation and reduction onset values [25].

2.7 Thermal Analyses

Thermal characterization and decomposition were determined by using TG–DTA and DSC. Thermal data were obtained by using Perkin Elmer Diamond Thermal Analysis. The TG–DTA measurements were made between 20 and 1,000 °C (in N_2, 10 °C/min). DSC analyses were carried out between 25 and 420 °C (in N_2, 20 °C/min) using Perkin Elmer Pyris Sapphire DSC. DMA tests were carried out by Perkin Elmer Pyris Diamond DMA 115 V. Rectangular samples of 10 mm (length) × 5.5 mm (width) × 0.6 mm (thickness) were used to conduct DMA tests in single cantilever bending mode at a frequency of 1 Hz, a heating rate of 3 °C/min and in the range 20–350 °C. The sample was prepared as follows: 0.5 g of PUs containing azomethine was placed into the titanium clamp (supplied from Triton Technology Ltd., United Kingdom) and extended followed by closing of the clamp from both sides by clamping.

2.8 Morphological Properties

Scanning electron microscopy (SEM) photographs of PUs containing azomethine were performed JSM-7001F/JSM-7001FA Thermal FE SEM. For SEM, PUs samples were sprinkled on double-sided adhesive tape mounted on an aluminum stub. Then they were coated with a thin gold/palladium film using sputter coater.

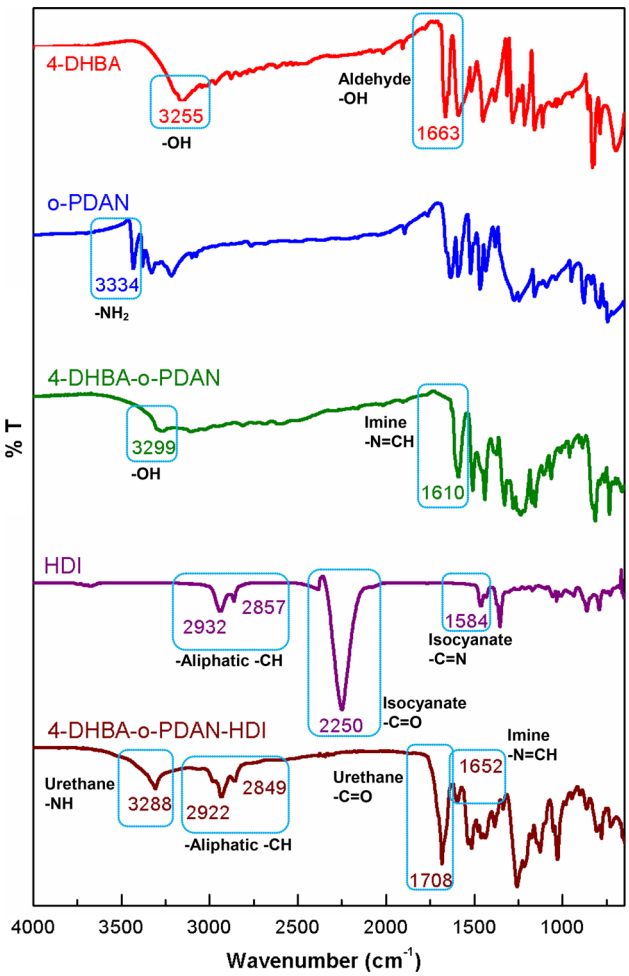

Fig. 1 FT-IR spectra of 4-DHBA, *o*-PDAN, 4-DHBA-*o*-PDAN, HDI and 4-DHBA-*o*-PDAN-HDI

Table 1 FT-IR spectrum data of the obtained compounds and starting compounds

Compounds	Urethane –NH	Urethane –C=O	Imine –N=CH	Isocyanate –C=O	Isocyanate –C=N	–OH	$-NH_2$	Aldehyde –CHO	Aromatic –CH	Aliphatic –CH	Aromatic –C=C
4-DBA	–	–	–	–	–	3,255	–	1,663	3,044	–	1,590, 1,516, 1,450
o-PDA	–	–	–	–	–	–	3,384	–	3,029	–	1,590, 1,526, 1,497
o-PDAM	–	–	–	–	–	–	3,434	–	3,029	2,912	1,594, 1,506, 1,456
o-PDAN	–	–	–	–	–	–	3,334	–	3,072	–	1,594, 1,522, 1,468
TDI	–	–	–	2,234	1,615	–	–	–	3,072	2,986	1,615, 1,574, 1,525
HDI	–	–	–	2,250	1,584	–	–	–	–	2,944	–
4-DHBA-*o*-PDA	–	–	1,611	–	–	3,255	–	–	3,026	–	1,542, 1,516, 1,481
4-DHBA-*o*-PDAM	–	–	1,613	–	–	3,309	–	–	3,026	2,967	1,542, 1,516, 1,474
4-DHBA-*o*-PDAN	–	–	1,610	–	–	3,299	–	–	3,035	–	1,592, 1,510, 1,470
4-DHBA-*o*-PDA-TDI	3,269	1,696	1,604	–	–	–	–	–	3,035	–	1,605, 1,544, 1,518
4-DHBA-*o*-PDAM-TDI	3,259	1,690	1,601	–	–	–	–	–	3,083	2,978	1,516, 1,440
4-DHBA-*o*-PDAN-TDI	3,318	1,717	1,659	–	–	–	–	–	3,026	–	1,514, 1,445
4-DHBA-*o*-PDA-HDI	3,353	1,740	1,656	–	–	–	–	–	3,090	2,977	1,513, 1,496, 1,442
4-DHBA-*o*-PDAM-HDI	3,310	1,685	1,597	–	–	–	–	–	3,082	2,981	1,512, 1,444
4-DHBA-*o*-PDAN-HDI	3,288	1,708	1,652	–	–	–	–	–	3,027	2,918	1,537, 1,514, 1,442

3 Results and Discussion

3.1 Characterization

4-DHBA-*o*-PDA, 4-DHBA-*o*-PDAM, 4-DHBA-*o*-PDAN are cream, brown and dark-red compounds, respectively. 4-DHBA-*o*-PDA-TDI, 4-DHBA-*o*-PDAM-TDI, 4-DHBA-*o*-PDAN-TDI, 4-DHBA-*o*-PDA-HDI, 4-DHBA-*o*-PDAM-HDI, 4-DHBA-*o*-PDAN-HDI are dark-brown, light brown, yellow, yellow, dark-red and brown compounds, respectively. According to solubility test results, PUs containing azomethine are completely soluble only in strong polar solvents like DMSO and DMF. They are partly soluble in THF and acetone whereas they are insoluble in MeOH, EtOH, ethyl acetate, MeCN, MeOH, $CHCl_3$ and CCl_4.

FT-IR, ^{1}H-NMR and ^{13}C-NMR data confirmed that Schiff bases and their PAMU derivatives were successfully synthesized. FT-IR spectra of 4-DHBA, *o*-PDAN,

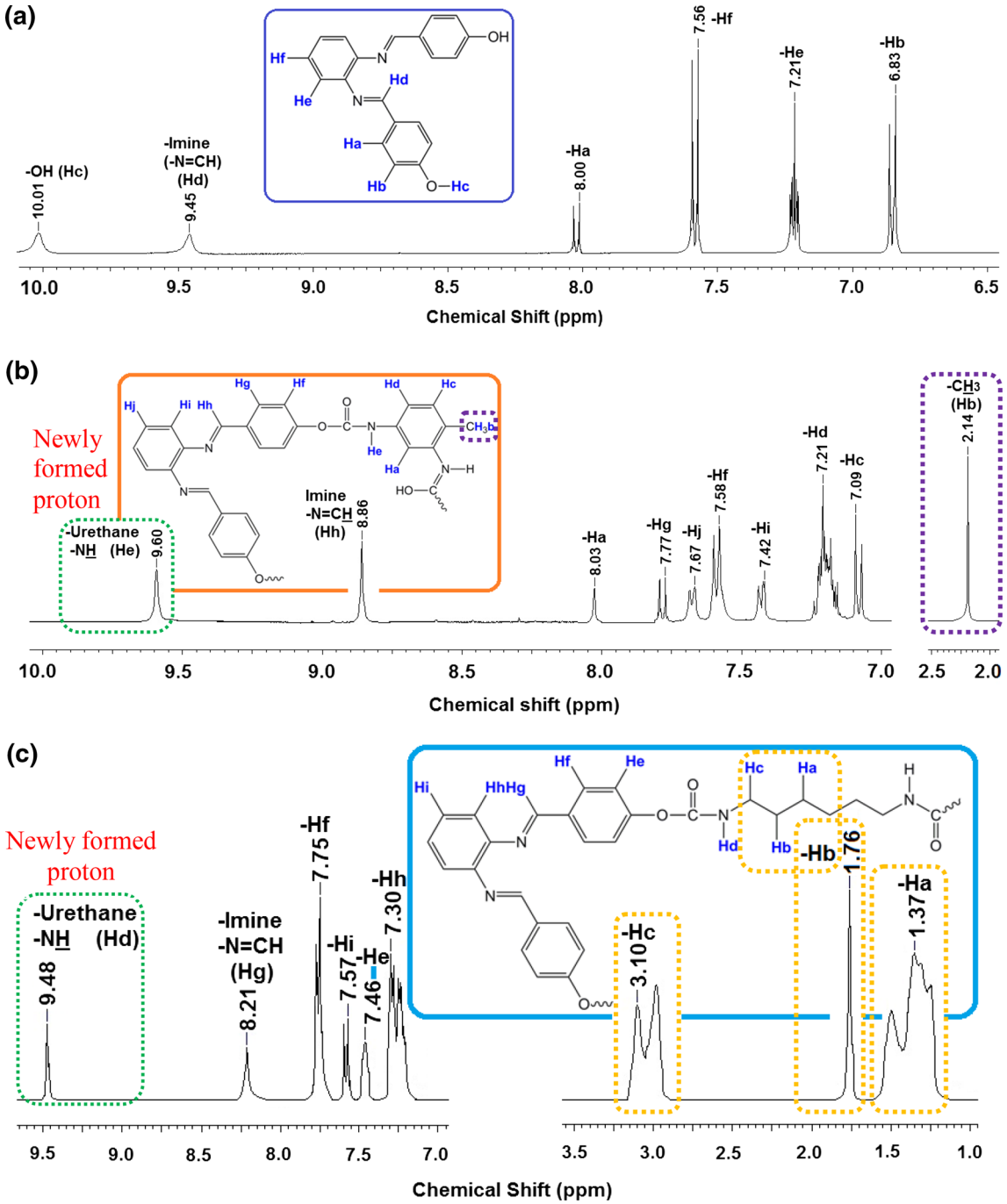

Fig. 2 ^{1}H-NMR spectra of 4-DHBA-*o*-PDA (**a**), 4-DHBA-*o*-PDA-TDI (**b**) and 4-DHBA-*o*-PDA-HDI (**c**)

4-DHBA-*o*-PDAN, HDI and 4-DHBA-*o*-PDAN-HDI are given in Fig. 1 and FT-IR spectral data all of the compounds summarized in Table 1. According to FT-IR spectra of 4-DHBA, characteristic aldehyde (–CHO) and hydroxyl (–OH) stretch vibrations are observed at 1,663 and 3,255 cm^{-1}, respectively. As can be seen in Table 1, characteristic amine ($–NH_2$) stretch vibration of *o*-PDAN is observed at 3,334 cm^{-1}. Similarly, characteristic $–NH_2$ stretch vibration of *o*-PDA and *o*-PDAM is observed at 3,384 and 3,434 cm^{-1}, respectively. According to the FT-IR spectra of 4-DHBA-*o*-PDAN, characteristic stretch vibrations for functional groups of reagents aldehyde and amine stretch vibrations were disappeared and imine (–N=CH) stretch vibration was formed. This newly formed –N=CH stretch vibration is observed at 1,611, 1,613 and 1,610 cm^{-1} for 4-DHBA-*o*-PDA, 4-DHBA-*o*-PDAM and 4-DHBA-*o*-PDAN, respectively. In addition, characteristic –OH stretch vibration of Schiff bases is observed between 3,255 and 3,309 cm^{-1}. As can be seen in Fig. 1, characteristic isocyanate –C=O and –C=N stretch vibrations of HDI are observed at 2,250 and 1,584 cm^{-1}, respectively, as in the literature [16]. Similarly, isocyanate –C=O and –C=N stretch vibrations of TDI are observed at 2,234 and 1,615 cm^{-1}, respectively, as in the literature [19]. According to Table 1, hydroxyl (–OH) stretch vibration of Schiff base, and isocyanate –C=O and –C=N stretch vibrations of TDI and HDI disappear due to urethane formation. Moreover, in the FT-IR spectra of 4-DHBA-*o*-PDAN-HDI the new stretch vibrations appear at 3,288 and 1,708 cm^{-1}, respectively, which could be attributed to urethane –NH and carbonyl (–C=O) stretch vibrations, respectively [26]. These newly formed stretch vibrations of the other PUs containing azomethine are observed between 3,259–3,353 and 1,685–1,740 cm^{-1}, respectively. Also, imine (–N=CH) stretch vibration of PUs is observed in the range 1,597–1,659 cm^{-1}.

Figure 2a–c show ^{1}H-NMR spectra of 4-DHBA-*o*-PDA, 4-DHBA-*o*-PDA-TDI and 4-DHBA-*o*-PDA-HDI, respectively.

Table 2 NMR spectra data of compounds

Compounds	Spectral data (δ_{ppm})
4-DHBA-*o*-PDA	^{1}H-NMR (DMSO): 10.01 (s, –OH, Hc), 9.45 (s, imine (–N=CH), Hd) 8.00 (d, Ha), 7.56 (d, Hf), 7.21 (m, He) and 6.83 (d, Hb)
	^{13}C-NMR (DMSO): 158.81 (–C–OH, C_3-ipso), 156.64 (imine, –N=CH, C_5–H), 142.69 (C_1–H), 135.83 (C_7–H), 130.59 (C_4), 127.49 (C_8–H), 120.80 (C_6–H) and 115.45 (C_2–H)
4-DHBA-*o*-PDAM	^{1}H-NMR (DMSO): 10.01 (s, –OH), 9.46 (s, imine (–N=CH)), 6.81–7.56 (aromatic –CH), 2.39 (t, $–CH_3$)
	^{13}C-NMR (DMSO): 158.71 (–C–OH), 156.61 (imine, (–N=CH)), 115.49–143.01 (aromatic –CH) and 21.45 ($–CH_3$)
4-DHBA-*o*-PDAN	^{1}H-NMR (DMSO): 9.77 (s, –OH), 8.39 (s, imine (–N=CH)) 6.69-8.07 (aromatic –CH)
	^{13}C-NMR (DMSO): 160.12 (–C–OH), 158.92 (imine, (–N=CH))), 117.63–147.29 (aromatic –CH)
4-DHBA-*o*-PDA-TDI	^{1}H-NMR (DMSO): 9.60 (s, urethane –NH, He), 8.86 (s, imine (–N=CH), Hh), 8.03 (s, Ha), 7.77 (d, Hg), 7.67 (d, Hj), 7.58 (d, Hf), 7.42 (d, Hi), 7.21 (m, Hd), 7.09 (d, Hc) and 2.14 (s, $–CH_3$, Hb)
	^{13}C-NMR (DMSO): 162.30 (imine, –N=CH, C_{13}–H), 158.92 (urethane, C_8=O), 156.67 (C_9-ipso), 142.67 (C_2-ipso), 137.17 (C_{12}), 136.44 (C_7), 132.11 (C_{15}–H), 130.60 (C_{11}–H), 130.25 (C_5–H), 128.18 (C_3), 127.49 (C_{16}–H), 127.10 (C_{14}), 121.89 (C_{10}–H), 118.91 (C_6–H), 115.47 (C_1–H) and 17.10 (C_4–H)
4-DHBA-*o*-PDAM-TDI	^{1}H-NMR (DMSO): 9.49 (s, urethane –NH), 8.45 (s, imine (–N=CH)), 6.45–8.13 (aromatic –CH), 2.52 (t, $–CH_3$) and 2.14 (t, $–CH_3$)
	^{13}C-NMR (DMSO): 162.76 (imine, –N=CH), 158.67 (urethane, –C=O), 105.53–152.30 (aromatic –CH), 22.52 ($–CH_3$) and 17.09 ($–CH_3$)
4-DHBA-*o*-PDAN-TDI	^{1}H-NMR (DMSO): 9.45 (s, urethane –NH), 7.96 (s, imine (–N=CH)), 6.67–7.73 (aromatic –CH), and 2.40 (t, $–CH_3$)
	^{13}C-NMR (DMSO): 162.30 (imine, –N=CH), 156.60 (urethane, –C=O), 105.09–153.09 (aromatic –CH) and 17.26 ($–CH_3$)
4-DHBA-*o*-PDA-HDI	^{1}H-NMR (DMSO): 9.48 (s, urethane –NH, Hd), 8.21 (s, imine (–N=CH), Hg), 7.75 (d, Hf), 7.57 (d, Hi), 7.46 (s, He), 7.30 (d, Hh), 3.10 (d, Hc), 1.76 (s, Hb) and 1.37 (d, Ha)
	^{13}C-NMR (DMSO): 158.84 (imine, C_9-H), 156.73 (Urethane, C_4=O), 153.84 (C_5-ipso), 135.84 (C_8), 130.18 (C_{11}-H), 136.44 (C_7), 127.51 (C_7-H), 122.12 (C_{12}-H), 119.51 (C_{10}-ipso), 115.50 (C_6-H), 47.07 (C_3-H), 30.03 (C_2-H) and 26.03 (C_1-H)
4-DHBA-*o*-PDAM-HDI	^{1}H-NMR (DMSO): 9.45 (s, urethane –NH), 8.17 (s, imine (–N=CH)), 6.82–7.56 (aromatic –CH), 2.52 (t, $–CH_3$) and 1.46–3.08 (aliphatic –CH)
	^{13}C-NMR (DMSO): 162.30 (imine, –N=CH), 158.78 (urethane, –C=O), 115.48–153.90 (aromatic –CH), 21.18 ($–CH_3$) and 26.09–35.78 (aliphatic –CH)
4-DHBA-*o*-PDAN-HDI	^{1}H-NMR (DMSO): 9.43 (s, urethane –NH), 7.96 (s, imine (–N=CH)), 7.22–7.55 (aromatic –CH), and 1.29–3.18 (aliphatic –CH)
	^{13}C-NMR (DMSO): 158.72 (imine, –N=CH), 156.61 (urethane, –C=O), 115.49–153.47 (aromatic –CH), and 21.18–35.78 (aliphatic –CH)

^{1}H-NMR spectral data all of the compounds were also summarized in Table 2. According to Fig. 2a, hydroxyl (–OH) and imine (–N=CH) protons of 4-DHBA-*o*-PDA are observed at 10.01 and 9.45 ppm, respectively. Similarly, hydroxyl (–OH) and imine (–N=CH) protons of 4-DHBA-*o*-PDAM and 4-DHBA-*o*-PDAN are observed at 10.01–9.77 and 9.46–8.39 ppm, respectively. In addition, aromatic protons of Schiff bases are observed in the range 6.69–8.07 ppm. As can be seen in Fig. 2b, c, urethane (–NH) and imine (–N=CH) protons of 4-DHBA-*o*-PDA-TDI and 4-DHBA-*o*-PDA-HDI are observed at 9.48–9.60 and 8.21–8.86 ppm, respectively. Similarly, urethane (–NH) and imine (–N=CH) protons of 4-DHBA-

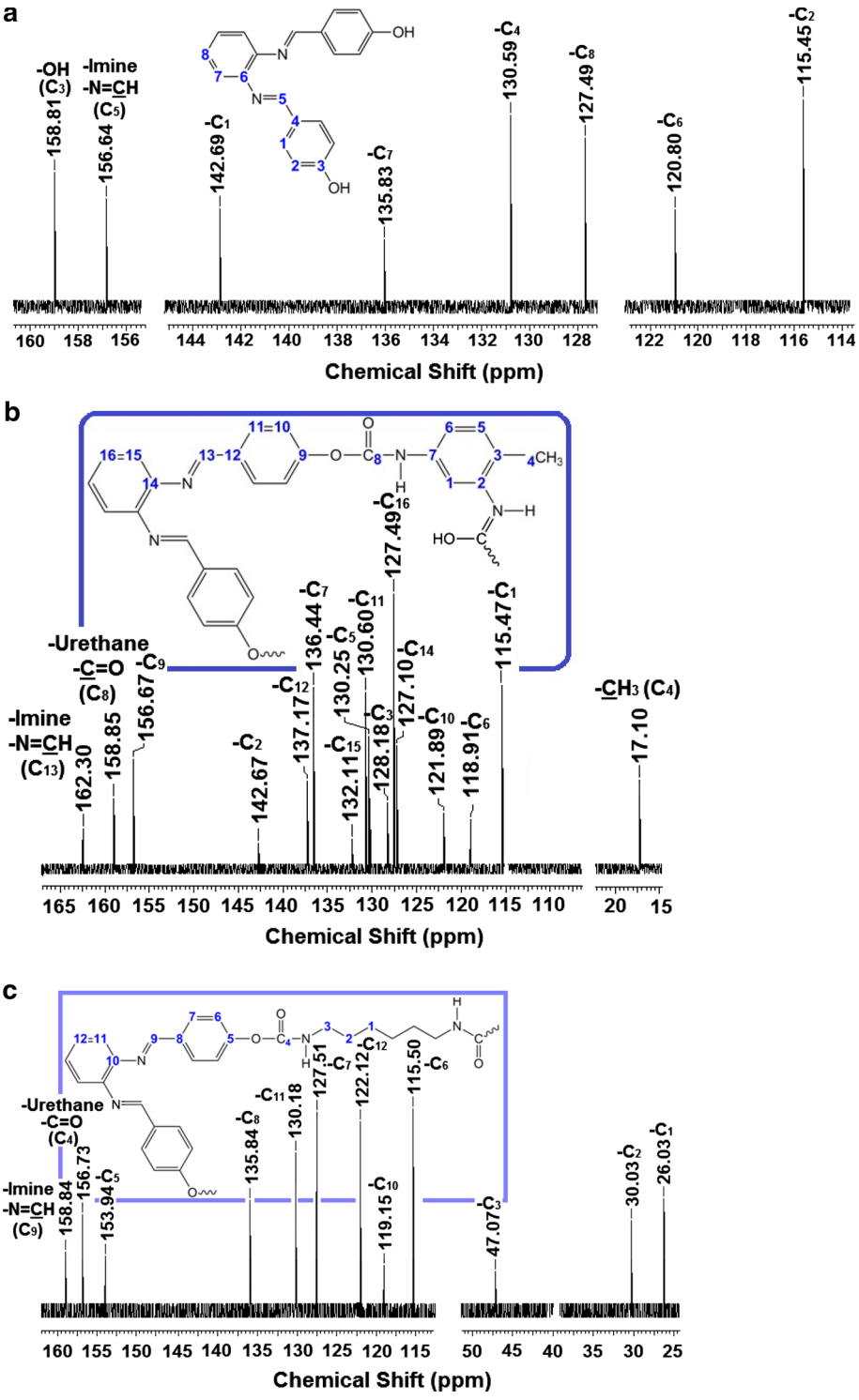

Fig. 3 ^{13}C-NMR spectra of 4-DHBA-*o*-PDA (**a**), 4-DHBA-*o*-PDA-TDI (**b**) and 4-DHBA-*o*-PDA-HDI (**c**)

o-PDAM-TDI, 4-DHBA-*o*-PDAN-TDI, 4-DHBA-*o*-PDAM-HDI and 4-DHBA-*o*-PDAN-HDI are observed in the range 9.43–9.49 and 7.96–8.45 ppm, respectively. In addition, aromatic protons of PUs containing azomethine are also observed between 6.45 and 8.13 ppm. Methyl (–$\underline{C}H_3$) proton of 4-DHBA-*o*-PDA-TDI, 4-DHBA-*o*-PDAN-TDI and 4-DHBA-*o*-PDAM-TDI is observed at 2.14, 2.40 and 2.14 ppm, respectively. Aliphatic protons of 4-DHBA-*o*-PDA-HDI, 4-DHBA-*o*-PDA-HDI and 4-DHBA-*o*-PDA-HDI resulting from aliphatic HDI are observed in the range 1.37–3.10 ppm.

Figure 3a, b and c show ^{13}C-NMR spectra of 4-DHBA-*o*-PDA, 4-DHBA-*o*-PDA-TDI and 4-DHBA-*o*-PDA-HDI, respectively. ^{13}C-NMR spectral data all of the compounds were also summarized in Table 2. According to Fig. 3a, hydroxyl (–$\underline{C}$–OH) and imine carbons (–N=$\underline{C}$H) of 4-DHBA-*o*-PDA are observed at 158.81 and 156.64 ppm, respectively. In addition, hydroxyl (–$\underline{C}$–OH) carbon of 4-DHBA-*o*-PDAM and 4-DHBA-*o*-PDAN are observed at 158.71 and 160.12 ppm and imine (–N=$\underline{C}$H) carbon of these compounds are observed at 156.61 and 158.92 ppm, respectively. As seen in Fig. 3b, c, hydroxyl carbon (–$\underline{C}$–OH) disappears due to urethane formation and imine (–N=$\underline{C}$H) carbon of 4-DHBA-*o*-PDA-TDI and 4-DHBA-*o*-PDA-HDI are observed at 162.30 and 158.84 ppm, respectively. According to the Table 2, this azomethine (–N=CH) carbon of the other PAMUs is observed in the range 158.72–162.76 ppm. ^{13}C-NMR spectra of PAMUs at Fig. 3b, c also confirm the structure by the peaks observed at 158.92 and 156.73 ppm, respectively, which could be attributed to the urethane carbon. According to Table 2, this peak of the other PAMUs is observed between 156.61 and 158.67 ppm. These results clearly show that the synthesized PAMUs are obtained with the proposed structures shown in Scheme 1.

3.2 Size Exclusion Chromatography

The average molecular weight of PUs containing azomethine was measured by SEC, using polystyrenes as standard and THF as eluent [27]. The number-average molecular weight (Mn), the weight-average molecular weight (Mw) and polydispersity index (PDI) values of PAMUs were measured by using RI detector (RID) [19]. The Mn, Mw and PDI values of PUs containing azomethine were calculated as 6,800, 8,400 and 1.235 for 4-DHBA-*o*-PDA-TDI, 7,250, 8,160 and 1.126 for 4-DHBA-*o*-PDAM-TDI, 11,700, 13,980 and 1.195 for 4-DHBA-*o*-PDAN-TDI, 9,800, 11,050 and 1.128 for 4-DHBA-*o*-PDA-HDI, 11,800, 12,700 and 1.076 for 4-DHBA-*o*-PDAM-HDI and 8,250, 10,800 and 1.309 for 4-DHBA-*o*-PDAN-HDI, respectively. According to the average molecular weight, 4-DHBA-*o*-PDA-TDI, 4-DHBA-*o*-PDAM-TDI, 4-DHBA-*o*-PDAN-TDI, 4-DHBA-*o*-PDA-HDI, 4-DHBA-*o*-PDAM-HDI and 4-DHBA-*o*-PDAN-HDI have nearly 22–27, 22–25, 32–39, 31–35, 35–38 and 23–30 repeated units, respectively.

3.3 Photophysical Properties

Photophysical properties of Schiff bases and PUs containing azomethine were investigated by using ultraviolet–visible (UV–Vis spectra) and photoluminescence (PL) spectroscopy. Figure 4 shows UV–Vis spectra of Schiff bases and PUs containing azomethine. It was found that 4-DHBA-*o*-PDAM showed one strong UV–Vis absorption maxima at 300 nm and 4-DHBA-*o*-PDAN showed two strong UV absorption maxima at 288 and 362 nm while

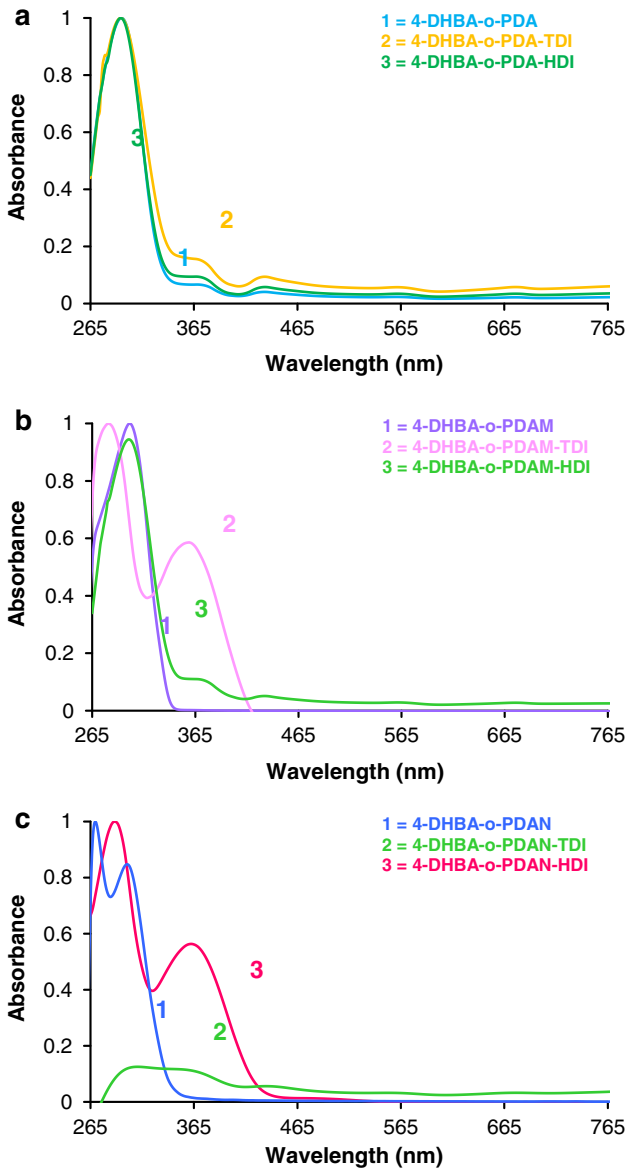

Fig. 4 UV–Vis spectra of 4-DHBA-*o*-PDA (**a**), 4-DHBA-*o*-PDAM (**b**), 4-DHBA-*o*-PDAN (**c**) and their PAMU derivatives

Table 3 Photophysical properties of PUs containing azomethine

Compounds	UV–Vis			PL					
	λ (nm)	λ_{onset} (nm)	E_g (eV)[a]	Conc. (mg/L)	λ^b_{Ex}	λ^c_{Em}	λ_{max} (absorption)	I^d_{max}	Stockes shift
4-DHBA-*o*-PDA	293, 368, 433	503	2.47	4.00×10^{-1}	351	365	382, 693	92, 56	31
4-DHBA-*o*-PDAM	300	340	3.65	8.00×10^{-1}	345	372	384, 696	953, 100	39
4-DHBA-*o*-PDAN	288, 362	347	3.58	1.25×10^{-2}	310	358	354, 703	223, 19	44
4-DHBA-*o*-PDA-TDI	294, 362, 436	553	2.25	4.00×10^{-1}	338	354	364, 695	981, 78	26
4-DHBA-*o*-PDAM-TDI	281, 357	437	2.84	2.50×10^{-2}	297	319	354, 598	45, 13	57
4-DHBA-*o*-PDAN-TDI	298, 370, 432	518	2.40	2.00×10^{-1}	352	372	417, 708	156, 22	65
4-DHBA-*o*-PDA-HDI	294, 372, 434	541	2.29	2.00×10^{-1}	332	357	415, 694	993, 813	83
4-DHBA-*o*-PDAM-HDI	300, 373, 435	496	2.50	1.25×10^{-2}	278	293	401, 715	995, 250	123
4-DHBA-*o*-PDAN-HDI	275, 299, 370	436	2.85	2.50×10^{-2}	339	356	368, 707	948, 84	29

[a] Optical band gap

[b] Excitation wavelength for emission

[c] Emission wavelength for excitation

[d] Maximum emission intensity

4-DHBA-*o*-PDA presented two small peaks at 368 and 433 nm and one strong UV–Vis absorption maximum at 293 nm. According to these results, 4-DHBA-*o*-PDA, 4-DHBA-*o*-PDAM and 4-DHBA-*o*-PDA presented one strong absorption maxima in the range of 288–300 nm corresponding to the $\pi \rightarrow \pi^*$ transitions of the azomethine linkage (–N=CH). In addition, 4-DHBA-*o*-PDAN exhibited one strong absorption maxima at 362 nm due to nitro group ($-NO_2$) in the structure. The small wavelength band originates in the electronic transition of the aromatic units. As seen in Scheme 1, PUs containing azomethine contain lone pairs of electron (–O and –N) and multiple bond (–CH=N–, –C=O, –C=C– and –N=O). These compounds exhibited maximum UV–Vis absorption at 281–300, 299–373 and 370–434 nm in DMSO as shown in Fig. 4, ascribed to the $\pi \rightarrow \pi^*$ transition of urethane linkage, $\pi \rightarrow \pi^*$ and $n \rightarrow \pi^*$ transitions of the azomethine linkage, respectively [26].

Optical band gap of Schiff bases and their PAMU derivatives were calculated as in the literature [24] and the obtained results were also summarized in Table 3. Optical band gap of 4-DHBA-*o*-PDA, 4-DHBA-*o*-PDAM and 4-DHBA-*o*-PDAN were calculated as 2.47, 3.65 and 3.58 eV, respectively. Additionally, optical band gap values of PUs containing azomethine found in the range 2.25–2.85 eV. The obtained results showed that PUs containing azomethine have lower optical band gap than their Schiff bases due to polyconjugated structures of the polymers [23].

Figure 5 shows fluorescence spectra of Schiff bases and their PAMU derivatives. Absorption–emission characteristic of Schiff bases and PUs containing azomethine have been studied in DMF and the obtained results were summarized in Table 3. According to the obtained results, Schiff bases and their PAMU derivatives have two emission maxima. The first emission maxima of Schiff bases showed that 4-DHBA-*o*-PDAM has the highest emission maxima (384 nm) while 4-DHBA-*o*-PDAN has the lowest emission maxima (354 nm) due to the structure of Schiff bases. As seen in Scheme 1, 4-DHBA-*o*-PDAM has methyl group ($-CH_3$) *o*- and *p*-position of azomethine bond while 4-DHBA-*o*-PDAN has nitro group ($-NO_2$) the same position. As known, methyl group is electron-donating group while nitro group is electron-withdrawing group. Also, $-CH_3$ group partly increases the electron density of *ortho* and *para* positions of the aromatic ring [8] while $-NO_2$ group decreases the electron density [28]. According to the PL spectra of PUs containing azomethine, they have two absorption maxima between 354–417 and 598–715 nm. The obtained results showed that 4-DHBA-*o*-PDA-HDI series have higher emission intensity than 4-DHBA-*o*-PDA-TDI series. This could be attributed because of polarity and dielectric constants of solvent and structure of PUs containing azomethine [29]. In addition, Stokes shift of Schiff bases were determined as 31, 39 and 44 nm for 4-DHBA-*o*-PDA, 4-DHBA-*o*-PDAM and 4-DHBA-*o*-PDAN, respectively. According to Stoke shift values of PU containing azomethine, they have in the range 26–123 nm Stokes shift values. According to Stokes shift values, PUs containing azomethine (except for 4-DHBA-*o*-PDA-TDI and 4-DHBA-*o*-PDAN-HDI) could be used as fluorescence sensor due to quite high Stokes shift value [21].

3.4 Electrochemical Properties

The electrochemical behaviors of Schiff bases and their PAMU derivatives are investigated by CV with a three-electrode electrochemical cell. The highest occupied

molecular orbital (HOMO), the lowest unoccupied molecular orbital (LUMO) and electrochemical band gap values of Schiff bases and their PAMU derivatives were calculated due to understand electronic structures of the synthesized materials. Figure 6 shows obtained cyclic voltommagrams of Schiff bases and PUs containing azomethines. Electrochemical onset potentials and electronic energy levels of PUs containing azomethine were also summarized in Table 4. According to Table 4, oxidation and reduction peak potentials of Schiff bases are recorded as 1.0965 and −0.9997 V for 4-DHBA-*o*-PDA, 1.1081 and −1.0586 V for 4-DHBA-*o*-PDAM and, 0.7901 and −1.4074 V for 4-DHBA-*o*-PDAN, respectively. These peak potentials of PUs containing azomethine are recorded in the range 0.9685 to 1.4844 V and −0.8589 to −0.7010 V, respectively.

HOMO–LUMO energy levels and the electrochemical band gaps (E_g') of the compounds are calculated as in the literature [25]. HOMO and LUMO energy levels of Schiff bases were determined as −5.49 and −3.39 eV for 4-DHBA-*o*-PDA, −5.50 and −3.33 eV for 4-DHBA-*o*-PDAM and −5.18 and −2.98 eV for 4-DHBA-*o*-PDAN, respectively. The obtained results showed that 4-DHBA-*o*-PDAN has the highest HOMO energy level while 4-DHBA-*o*-PDAM has the lowest HOMO energy level. This could be probably structures of Schiff bases. As seen in Scheme 1, 4-DHBA-*o*-PDAM contains methyl (–CH_3) group as electron-donating group in the structure whereas 4-DHBA-*o*-PDAN contains nitro (–NO_2) group as electron-withdrawing group in the structure. As known, electron-donating groups partly increase the electron density of *ortho* and *para* positions of the aromatic ring, and they may extend the conjugation [30]. According to the calculated electrochemical band gap values of the materials, Schiff bases have in the range 2.10–2.20 eV electrochemical band gap and containing azomethine (except for 4-DHBA-*o*-PDAM-HDI) have below 2.0 eV electrochemical band gap. CV results showed that PUs containing azomethine are p-type conjugated polymers due to they have below −5.10 eV HOMO energy level, in the range—4.00 to −3.50 eV LUMO energy level and between 1.67 and 1.92 eV (except for 4-DHBA-*o*-PDAM-HDI) electrochemical band gap [30].

3.5 Thermal Analyses

Thermogravimetric analysis (TGA) of Schiff bases and their PAMU derivatives was carried out in N_2 in order to investigate their thermal stability and thermal degradation behavior. Figure 7a shows TG curves of 4-DHBA-*o*-PDAM, 4-DHBA-*o*-PDAM-TDI and 4-DHBA-*o*-PDAM-HDI. In addition, the TG–DTA data all of the Schiff bases and their polymers are also summarized in Table 5. TG–DTA results showed that Schiff bases and PUs containing azomethine decompose in three step except for 4-DHBA-*o*-PDA, 4-DHBA-*o*-PDA-TDI and 4-DHBA-*o*-PDAN-HDI. 4-DHBA-*o*-PDA decomposes in a single step while 4-DHBA-*o*-PDA-TDI and 4-DHBA-*o*-PDAN-HDI decompose in two-step.

In the first degradation step (in the range 125–340 °C), thermally labile urethane component of PUs containing azomethine decomposes isocyanate and alcohol [31]. The second and third degradation steps of the PAMUs correspond to the decomposition of alcohol by dehydration [32]. According to TG data of Schiff bases, the onset temperature

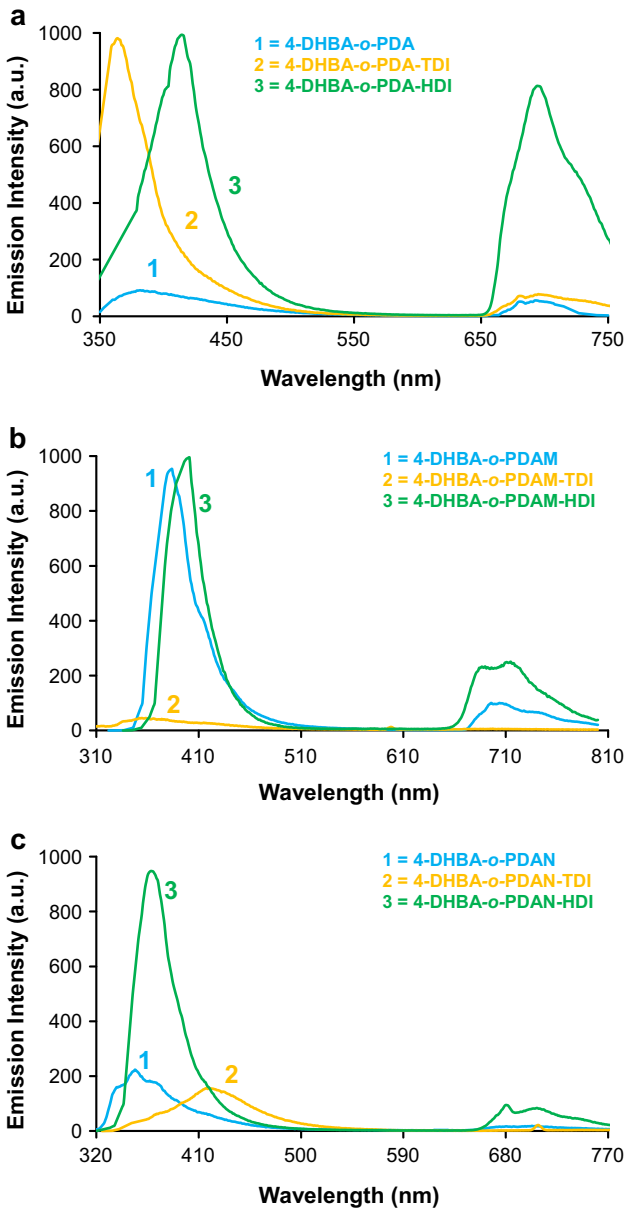

Fig. 5 Fluorescence spectra of 4-DHBA-o-PDA (a), 4-DHBA-o-PDA (b), 4-DHBA-o-PDA (c) and their PAMU derivatives

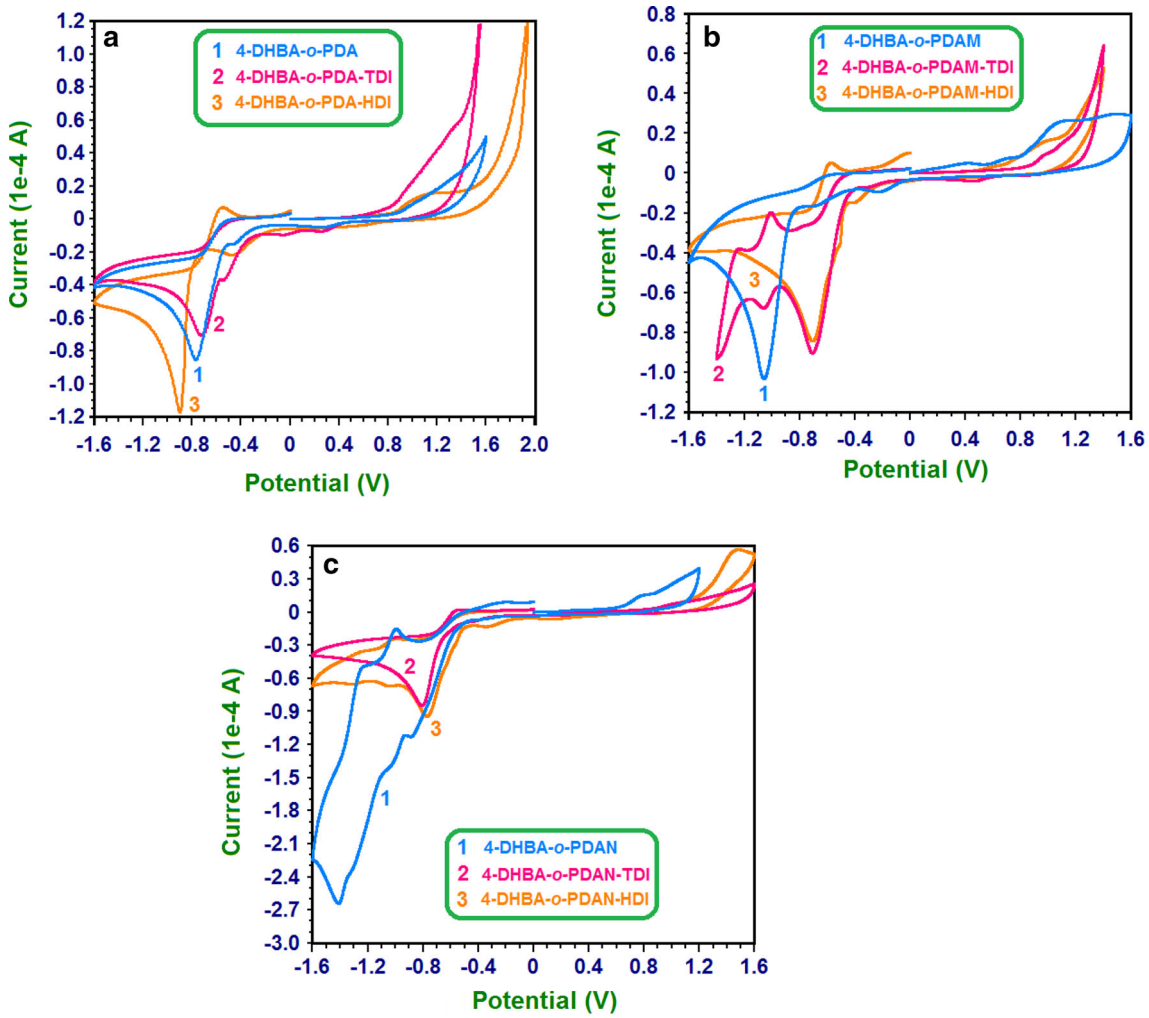

Fig. 6 Cyclic voltammograms of Schiff bases and PUs containing azomethine

Table 4 Electrochemical onset potentials and electronic energy levels of PUs containing azomethine

Compounds	E_{ox} (V)	HOMO (eV)[a]	E_{red} (V)	LUMO (eV)[b]	E'_g (eV)[c]
4-DHBA-*o*-PDA	1.0965	−5.49	−0.9997	−3.39	2.10
4-DHBA-*o*-PDAM	1.1081	−5.50	−1.0586	−3.33	2.17
4-DHBA-*o*-PDAN	0.7901	−5.18	−1.4074	−2.98	2.20
4-DHBA-*o*-PDA-TDI	0.9685	−5.36	−0.7010	−3.69	1.67
4-DHBA-*o*-PDAM-TDI	0.9865	−5.38	−0.7019	−3.69	1.69
4-DHBA-*o*-PDAN-TDI	1.0219	−5.41	−0.8077	−3.58	1.83
4-DHBA-*o*-PDA-HDI	1.0566	−5.45	−0.8589	−3.53	1.92
4-DHBA-*o*-PDAM-HDI	1.4844	−5.87	−0.7646	−3.63	2.25
4-DHBA-*o*-PDAN-HDI	0.9946	−5.38	−0.7019	−3.69	1.70

[a] Highest occupied molecular orbital

[b] Lowest unoccupied molecular orbital

[c] Electrochemical band gap

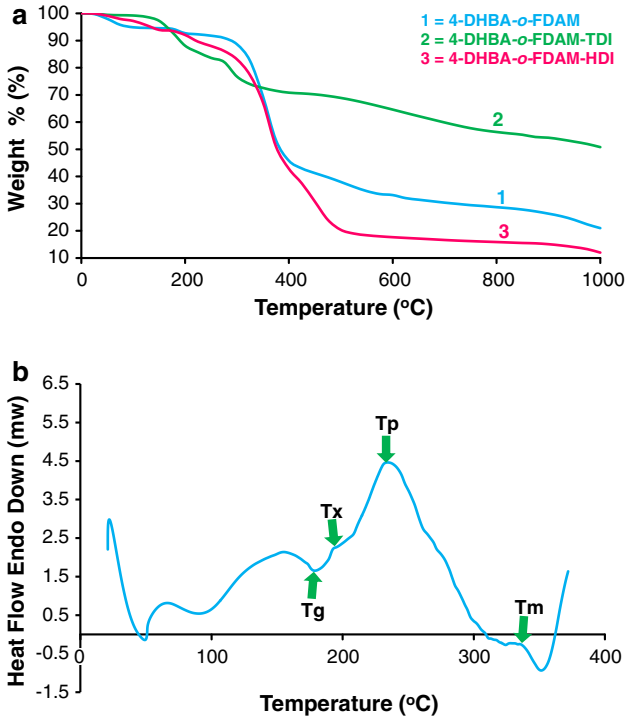

Fig. 7 TG curves of 4-DHBA-*o*-PDAM, 4-DHBA-*o*-PDAM-TDI and 4-DHBA-*o*-PDAM-HDI (**a**), and DSC curve of 4-DHBA-*o*-PDAN-TDI (**b**)

of 4-DHBA-*o*-PDA, 4-DHBA-*o*-PDAM and 4-DHBA-*o*-PDAN were determined as 316, 181 and 136 °C, respectively. This temperature of PU containing azomethine was determined in the range 125–263 °C. %20 (T20) and %50 (T50) weight loss and char at 1,000 °C were determined as 326 °C, 371 °C and 16.20 % for 4-DHBA-*o*-PDA, 326 °C, 378 °C and 21.00 % for 4-DHBA-*o*-PDAM and, 432 °C and 56.30 % for 4-DHBA-*o*-PDAN, respectively. T20, T50 and char values of PAMUs were determined in the range 245–316 °C, 357–697 °C and 10.90–50.80 %, respectively. Obtained results from char at 1,000 °C showed that 4-DHBA-*o*-PDA-TDI series have higher char than 4-DHBA-*o*-PDA-HDI series. This could be probably structures of PUs. As seen in Scheme 1, 4-DHBA-*o*-PDA-TDI series were fully synthesized aromatic compounds whereas 4-DHBA-*o*-PDA-HDI series were synthesized both aromatic compounds and aliphatic compounds. As known, aromatic compounds have higher thermal stability than aliphatic compounds [19].

The glass transition temperature (T_g), the crystallization temperature (T_x), the crystallization peak temperature (T_p) and the melting temperature (T_m) of PU containing azomethine were determined by DSC. DSC curve of 4-DHBA-*o*-PDAN-TDI is shown in Fig. 7b. In addition, the obtained results all of PUs are summarized in Table 6. According to the obtained results, PUs containing azomethine have in the range 110–171 °C the glass transition temperature (T_g), 124–284 °C the crystallization temperature (T_x), 147–352 °C the crystallization peak temperature (T_p) and 195–371 °C the melting temperature (T_m). These results clearly indicated that PUs containing azomethine exhibited semi-crystalline behavior due to they have crystallization temperature, crystallization peak temperature and melting temperature [19].

DMA analysis of polymer samples was carried out to investigate mechanical properties of polymers. The storage modulus (E′) and loss factor (tan δ) curves of PU containing azomethine are shown in Figs. 8 and 9, respectively. In DMA experiments, two parameters are used to characterize the viscoelastic properties of PUs containing azomethine. These are storage modulus (E′) and tan δ. E′ which reflects material stiffness and tan δ which also describes the damping properties or the ratio of viscous to elastic behavior [33].

According to the storage modulus (E′) of PUs, there are two characteristics region in E′ curves. These are glass region and glassy-transition region [34]. As seen Fig. 8, E′ curves show a linear portion in the region between 50 and 100 °C for 4-DHBA-*o*-PDA-TDI, 30 and 120 °C for 4-DHBA-*o*-PDAM-TDI, 30 and 65 °C for 4-DHBA-*o*-PDAN-TDI, 45 and 115 °C for 4-DHBA-*o*-PDA-HDI, 30 and 50 °C for 4-DHBA-*o*-PDAM-HDI and 30 and 145 °C for 4-DHBA-*o*-PDAN-HDI, where the variation of the modulus is less intense. This area is denominated glass region and it can be characterized by the low mobility of the polymeric chains. With the increase of the temperature, a steeper fall in the E′ modulus is also observed and it characterized the glassy-transition region.

Figure 9 shows Tan δ curves of PUs containing azomethine and obtained T_g values from these curves are also summarized in Table 6. The T_g of PUs were found between 122 and 213 °C. When compared to glass-transition temperature obtained from DMA and DSC, T_g values obtained from DMA have a bit higher than obtained from DSC (except for 4-DHBA-*o*-PDAN-TDI). This could be the different nature of these two methods. As known, DMA measures the change in the mechanical response of the polymer chains, while DSC measures the change in heat capacity from frozen to unfrozen chains [35].

3.6 Morphological Properties

Morphological properties of PUs containing azomethine are evaluated by using SEM. This technique was carried out to investigate surface morphology of PUs containing azomethine. The samples were prepared by putting a

Table 5 Thermal degradation values of the compounds

Compounds	First degradation temperature (°C)				Second degradation temperature (°C)				Third degradation temperature (°C)							
	T_{on}^{a}	$W_{max}T^{b}$	T_{end}^{c}	Percentage of weight loss	T_{start}^{d}	$W_{max}T^{b}$	T_{end}^{c}	Percentage of weight loss	T_{start}^{d}	$W_{max}T^{b}$	T_{end}^{c}	Percentage of weight loss	T_{20}^{e}	T_{50}^{f}	Char at 1,000 °C (%)	Lost of absorbed water or organic solvent (%)
4-DHBA-*o*-PDA	316	363	1,000	78.10	–	–	–	–	–	–	–	–	326	371	16.20	5.70
4-DHBA-*o*-PDAM	181	188	222	1.60	222	353	461	52.30	461	519	1,000	19.40	326	378	21.00	5.70
4-DHBA-*o*-PDAN	136	155	214	4.30	214	347	469	16.10	469	730	1,000	20.70	432	–	56.30	1.60
4-DHBA-*o*-PDA-TDI	182	233	272	22.50	272	362	1,000	58.80	–	–	–	–	245	361	16.30	2.40
4-DHBA-*o*-PDAM-TDI	152	173	211	8.30	211	294	420	14.80	420	622	1,000	24.60	289	–	50.80	1.50
4-DHBA-*o*-PDAN-TDI	141	199	239	11.70	239	294	382	21.50	382	450	1,000	22.80	277	697	41.30	2.70
4-DHBA-*o*-PDA-HDI	125	141	172	4.20	172	361	418	51.20	418	456	1,000	31.80	304	367	10.90	1.90
4-DHBA-*o*-PDAM-HDI	170	211	248	9.90	248	361	417	48.90	417	453	1,000	27.00	316	379	12.00	2.20
4-DHBA-*o*-PDAN-HDI	263	292	337	35.80	337	360	1,000	39.80	–	–	–	–	274	357	20.10	4.30

[a] The onset temperature

[b] Maximum weight temperature

[c] Final thermal degradation temperature

[d] Start thermal degradation temperature

[e] 20 % weight loss

[f] 50 % weight loss

Table 6 DMA and DSC data of PUs containing azomethine

Compounds	DMA	DSC				
	T_g (°C)[a]	T_g (°C)[a]	T_x (°C)[b]	T_p (°C)[c]	T_m (°C)[d]	ΔCp (J/g K)[e]
4-DHBA-*o*-PDA-TDI	122	110	124	147	195	0.003
4-DHBA-*o*-PDAM-TDI	139	138	147	170	220	0.086
4-DHBA-*o*-PDAN-TDI	144	171	192	231	325	0.011
4-DHBA-*o*-PDA-HDI	151	128	189	260	302	0.033
4-DHBA-*o*-PDAM-HDI	207	169	284	352	371	0.144
4-DHBA-*o*-PDAN-HDI	213	154	250	307	347	0.037

[a] The glass transition temperature

[b] The crystallization temperature

[c] The peak crystallization temperature

[d] The melting point

[e] Change of specific heat during glass transition

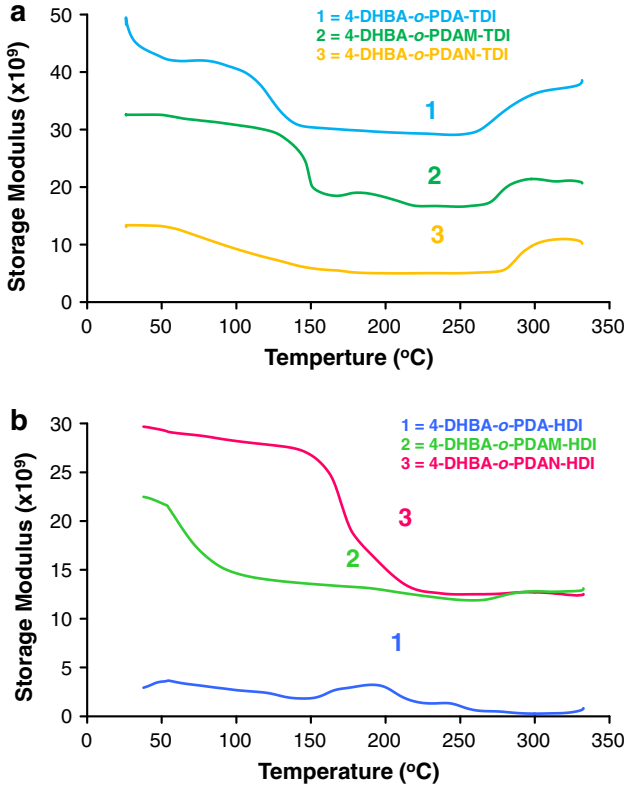

Fig. 8 Storage modulus curves of 4-HBA-*o*-PDA-TDI series (**a**) and 4-HBA-*o*-PDA-TDI series (**b**)

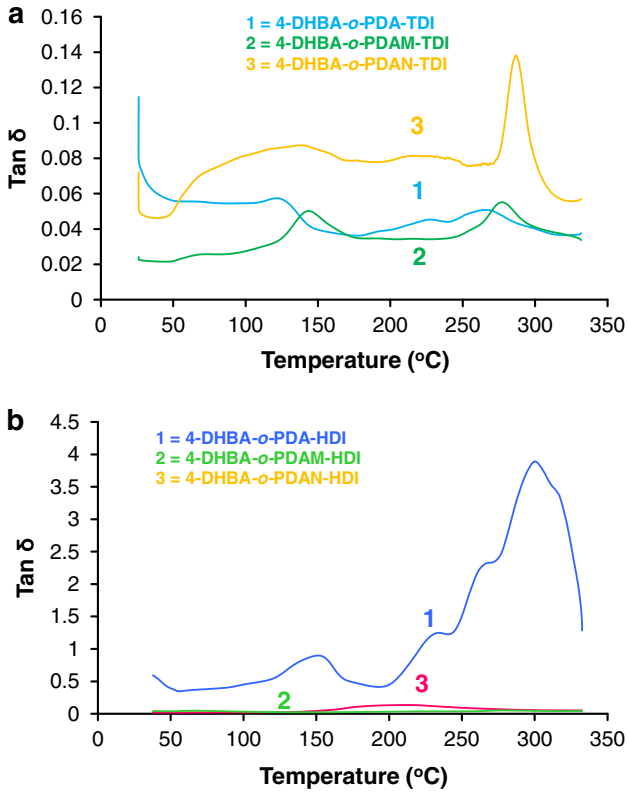

Fig. 9 Tan δ curves of 4-HBA-*o*-PDA-TDI series (**a**) and 4-HBA-*o*-PDA-TDI series (**b**)

smooth part of polymer powder on an aluminum holder and subsequently coating it with gold/palladium alloy.

Figure 10 shows SEM photographs of PUs at powder form. According to SEM images of polymers, they have different particle size and consist of semi-crystalline layers. As seen in Fig. 10, 4-DHBA-*o*-PDA-TDI and 4-DHBA-*o*-PDAM-HDI consist of rod-shaped semi-crystalline particles.

4 Conclusions

New low-band gap Schiff bases containing various side-group substitutions and PUs containing azomethine were successfully synthesized. The structures of the compounds

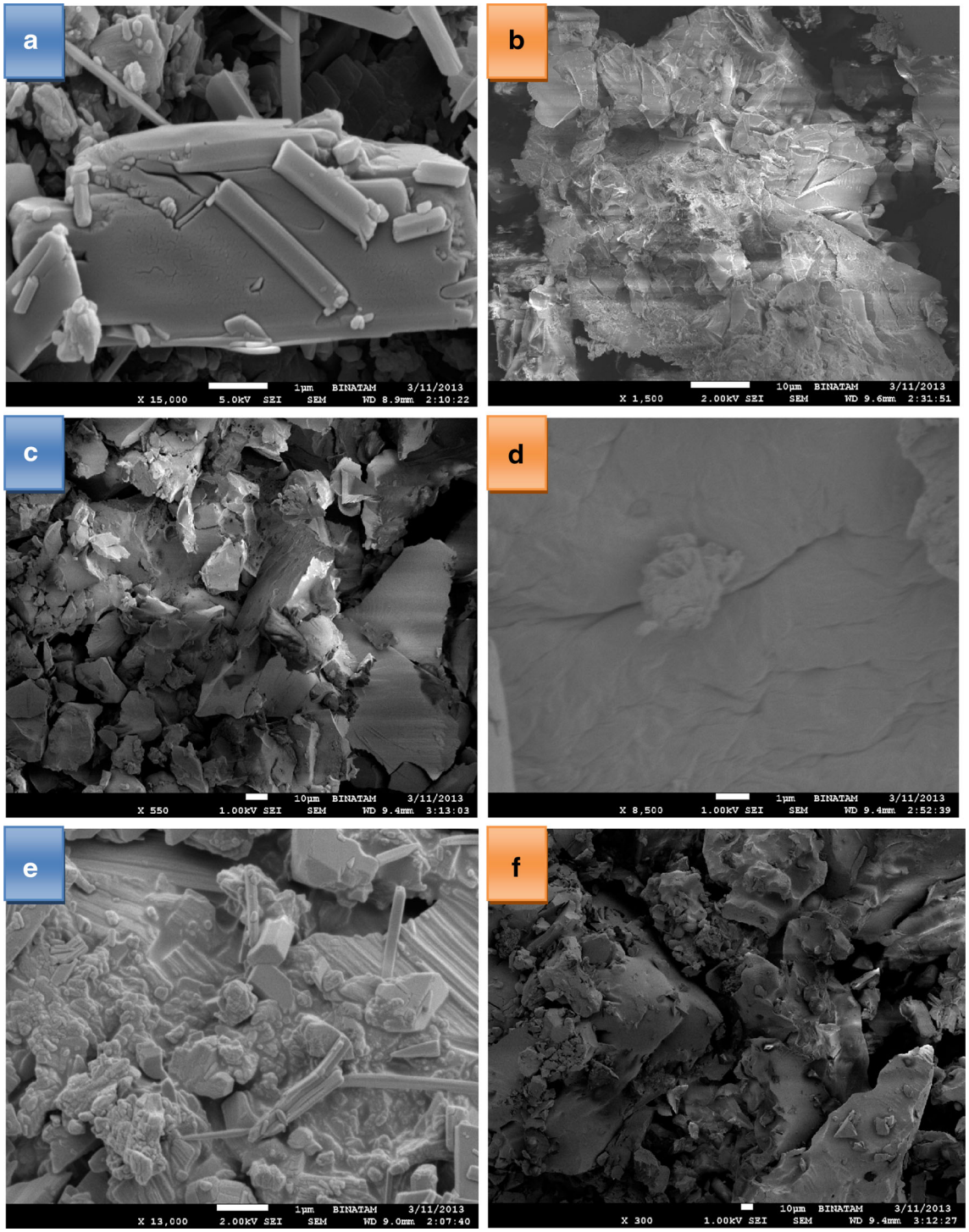

Fig. 10 SEM micrographs of 4-DHBA-*o*-PDA-TDI (**a**), 4-DHBA-*o*-PDAM-TDI (**b**), 4-DHBA-*o*-PDAN-TDI (**c**), 4-DHBA-*o*-PDA-HDI (**d**), 4-DHBA-*o*-PDAM-HDI (**e**) and 4-DHBA-*o*-PDAN-HDI (**f**)

were clarified by using FT-IR, NMR, and SEC techniques. Photophysical properties of the synthesized compounds were investigated by UV–Vis and PL spectroscopy. According to the optical band gap of PUs containing azomethine, they have in the range 2.25–2.85 eV optical band gap. In addition, Stokes shift of PUs found in the range 26–123 nm. Due to quite high Stokes shift value of PUs containing azomethine could be used as fluorescence sensor. Electrochemical properties were illuminated by using CV. CV results showed that PAMUs have below 2.0 eV electrochemical band gap. Due to this property, they could be used in heterojunction solar cells. DSC curves showed

that PUs contain both the crystallization and the melting peak. Because of these peaks, they are semi-crystalline materials. Morphological properties of the PAMUs were investigated by SEM. SEM photographs showed that PUs consist of semi-crystalline particles.

References

1. A. Pron, P. Rannou, Prog. Polym. Sci. **27**, 135 (2002)
2. K.W. Tsai, T.F. Guo, K.Y.A. Jen, T.C. Wen, J. Mat. Chem. C **2**, 272 (2014)
3. C. Reanprayoon, J. Gasiorowski, M. Sukwattanasinitt, N.S. Sariciftci, P. Thamyongkit, RSC Adv. **4**, 3045 (2014)
4. R. Kim, P.S.K. Amegadze, I. Kang, H.J. Yun, Y.Y. Noh, S.K. Kwon, Y.H. Kim, Adv. Funct. Mater. **23**, 5719 (2013)
5. S. Kola, J. Sinha, H.E. Katz, J. Polym. Sci., Part B: Polym. Phys. **50**, 1090 (2012)
6. M. Grigoras, C.O. Catanescu, J. Macromol. Sci. C Polym. Rev. **44**, 1 (2004)
7. İ. Kaya, M. Yıldırım, A. Aydın, D. Senol, React. Funct. Polym. **70**, 815 (2010)
8. İ. Kaya, M. Kamacı, F. Arıcan, J. Appl. Polym. Sci. **125**, 608 (2012)
9. İ. Kaya, A. Bilici, M. Saçak, J. Inorg. Organomet. Polym. **19**, 443 (2009)
10. L. Marin, E. Perju, M.D. Damaceanu, Eur. Polym. J. **47**, 1284 (2011)
11. G.T. Howard, Int. Biodeter. Biodegr. **49**, 245 (2002)
12. O.G. Armagan, B.K. Kayaoglu, H.C. Karakas, F.S. Guner, J. Ind. Textil. **43**, 396 (2014)
13. M. Sponton, N. Casis, P. Mazo, B. Raud, A. Simonetta, L. Rios, D. Estenoz, Int. Biodeter. Biodegr. **85**, 85 (2013)
14. V. Jaso, J. Milic, V. Divjakovic, Z.S. Petrovic, Eur. Polym. J. **49**, 3947 (2013)
15. H.Y. Mi, X. Jing, M.R. Salick, T.M. Cordie, X.F. Peng, L.S. Turng, J. Mater. Sci. **49**, 2324 (2014)
16. İ. Kaya, M. Kamacı, J. Appl. Polym. Sci. **125**, 876 (2012)
17. Gh Stoica, A. Stanciu, V. Cozan, A. Stoleriu, D. Timpu, J. Macromol. Sci. A **35**, 539 (1998)
18. I. Ali, S.M. Al-Zahrani, S.K. Dolui, Polym. Sci. Ser. B **54**, 342 (2012)
19. İ. Kaya, M. Kamacı, Prog. Org. Coat. **74**, 204 (2012)
20. A. Shanavas, M. Vanjinathan, A.S. Nasar, S. Amudha, S.A. Suthanthiraraj, High Perform. Polym. **24**, 561 (2012)
21. İ. Kaya, M. Kamacı, J. Fluoresc **23**, 115 (2013)
22. İ. Kaya, M. Yıldırım, M. Kamacı, Synthetic Met. **161**, 2036 (2011)
23. M. Kamacı, İ. Kaya, J. Inorg. Organomet. Polym. **23**, 1159 (2013)
24. M. Yıldırım, İ. Kaya, Synthetic Met. **162**, 834 (2012)
25. A. Avcı, K. Şirin, Des. Monomers Polym. **17**, 380 (2014)
26. K.R. Reddy, A.V. Raghu, H.M. Jeong, Polym. Bull. **60**, 609 (2008)
27. A. Bilici, F. Doğan, M. Yıldırım, İ. Kaya, J. Phys. Chem. C **116**, 19934 (2012)
28. C. Albayrak, G. Kastas, M. Odabasoglu, R. Frank, Spectrochim. Acta A **114**, 205 (2013)
29. M. Kamacı, İ. Kaya, Polym. Eng. Sci. **54**, 1664 (2014)
30. A. Pron, M. Leclerc, Progr. Polym. Sci. **88**, 1815 (2013)
31. P.S.G. Krishnan, C.Z. Cheng, Y.S. Cheng, J.W.C. Cheng, Macromol. Mater. Eng. **288**, 730 (2003)
32. D.K. Chattopadhyay, D.C. Webster, Progr. Polym. Sci. **34**, 1068 (2009)
33. F. Touaiti, M. Pahlevan, R. Nilsson, P. Alam, M. Toivakka, M.P. Ansell, C.E. Wilen, Prog. Org. Coat. **76**, 101 (2013)
34. J.A.F.F. Rocco, J.E.S. Lima, V.L. Lourenco, N.L. Batista, E.C. Botelho, K. Iha, J. Appl. Polym. Sci. **126**, 1461 (2012)
35. Y. Lu, R.C. Larock, Prog. Org. Coat. **69**, 31 (2010)